

# Characterization of chip formation during machining 1045 steel

Yang Qibiao · Liu Zhanqiang · Wang Bing

Received: 13 December 2011 / Accepted: 24 January 2012 / Published online: 11 February 2012  
© Springer-Verlag London Limited 2012

**Abstract** A deep understanding of the generation and characterization of chip formation can result for practical advices of chip type controlling in engineering applications. The chip formation is divided into the continuous chip and the serrated one in this study. The characterization of the continuous chip formation is expressed as the chip deformation and that of the serrated chip formation is expressed as the frequency of serration, the degree of segmentation, and the deformation of serrated chip. The chips of 1045 steel under different cutting speeds (100–3,600 m/min) are collected during machining. After inlay and polishing of the collected chips, the chip morphology is observed with VHX-600 ESO digital microscope. It is found that at the cutting speeds of 100–400 m/min, the chip type is continuous, at the cutting speeds of 600–2,200 m/min the chip type is serrated, and at the cutting speeds of 2,500–3,600 m/min the chip type is segmented. The quantitative relations between the characterization parameters of chip formation and the cutting speed are obtained. The chip deformation increases with the cutting speed, and the influence of the cutting speed on the shear strain rate is more sensitive than that on the shear strain during the continuous chip formation. All the characterization parameters including the shear strain rate, the frequency of serration, the degree of segmentation, and the shear strain increase with the cutting speed during the serrated chip formation. The sensitivity of influence of the cutting speed on these parameters is in the following: the shear strain rate, the degree of segmentation, the frequency of serration, and the shear strain.

**Keywords** Chip formation · Machining · Chip characterization · Chip deformation · 1045 steel

## 1 Introduction

There is a highly localized deformation during the chip formation of cutting process in the shear zone connecting the tool tip and the workpiece surface (primary deformation zone), and along the interface between the chip and the tool rake face (secondary shear zone) [1–3]. Within the shear zone, the workpiece material is deformed in a very short time interval and caused a large temperature rise. For example, during machining 1045 steel at a cutting speed of 300 m/min, the shear strain reaches to more than 1 and the shear strain rate reaches to the magnitude of  $10^5 \text{ s}^{-1}$  [4]. Furthermore, many observations show that with the cutting speed, increasing the chip type will be changed from the continuous chip to the serrated one [5–15]. This phenomenon may lead to high-frequency fluctuations of cutting force, accelerating the wear rate of cutting tool, reducing the machined surface quality and the machining accuracy [16]. For these reasons, it is necessary to study the mechanism of chip formation in machining process. Study on the characterization of chip formation can result for practical advices of controlling the chip type in engineering applications.

Schulz and Abele [17] have used the degree of segmentation to characterize the serrated chip of high-speed machining aluminum alloy 7075. The results indicate that the degree of segmentation increases with the cutting speed and the feed per tooth. Based on Aifantis [18], the deformation internal length and the thermal internal length are applied to measure the degree of segmentation [19]. The relationships between the deformation internal length, the thermal internal

Y. Qibiao · L. Zhanqiang (✉) · W. Bing  
School of Mechanical Engineering, Shandong University,  
Jinan 250061, China  
e-mail: melius@sdu.edu.cn

length, and shear band width are studied through the linear perturbation analysis. Molinari et al. [20] have proposed a model including the space of adiabatic shear band, the adiabatic shear band width, and the frequency of serration to characterize the serrated chip formation. Through the linear perturbation analysis, the analytic solutions of these parameters are obtained [21, 22]. The results show that the space of adiabatic shear band decreases with the cutting speed increasing [23–27] and the frequency of serration increases with the cutting speed.

1045 steel is a commonly used and high-quality carbon structural steel. However, the characterization of the chip formation during high-speed machining 1045 steel is still less involved. In order to study the characterization of chip formation and the differences of chip formation between the high-speed machining and conventional machining 1045 steel, in this paper, the characterization of chip formation classified as the continuous and serrated chip formation is studied. The experiment of machining 1045 steel under the heat treatment of quenching is performed. Some results in the investigation of the cutting speed influence on chip formation are presented. The quantitative relations between the characterization parameters and the cutting speed are built.

## 2 Characterization of chip formation

### 2.1 Characterization of continuous chip formation

The characterization of continuous chip formation is the deformation in the chip. It can be expressed as the chip deformation that is the shear strain and the shear strain rate.

The deformation coefficient  $\xi$  can be expressed as Eq. 1.

$$\xi = \frac{a_{\text{ch}}}{a_c} \quad (1)$$

where  $a_{\text{ch}}$  is the chip thickness and  $a_c$  is the uncut chip thickness. The shear strain and shear strain rate are usually expressed as Eqs. 2 and 3.

$$\gamma = \frac{\cos \gamma_0}{\sin \varphi \cos(\varphi - \gamma_0)} \quad (2)$$

$$\dot{\gamma} = \frac{\gamma V \sin \varphi}{s} \quad (3)$$

where  $\gamma$  is the shear strain,  $\gamma_0$  is the tool rake angle,  $\varphi$  is the shear angle,  $\dot{\gamma}$  is the shear strain rate,  $V$  is the cutting speed, and  $s$  is the thickness of the shear zone which can be expressed as Eq. 4 [28].

$$s = \frac{a_c}{5.9 \sin \varphi} \quad (4)$$

The shear angle  $\varphi$  can be expressed as Eq. 5:

$$\tan \varphi = \frac{\cos \gamma_0}{\xi - \sin \gamma_0} \quad (5)$$

Submitting Eq. 4 into Eqs. 3 and 6 can be obtained.

$$\dot{\gamma} = \frac{5.9V \sin \varphi \cos \gamma_0}{a_c \cos(\varphi - \gamma_0)} \quad (6)$$

### 2.2 Characterization of serrated chip formation

The mechanism of serrated chip formation during high-speed machining plastic metallic material can be regarded as catastrophic thermoplastic shear instability [29, 30]. The characterization of serrated chip is expressed as the frequency of serration, the degree of segmentation, and the deformation of serrated chip.

It is an assumption that a serrated chip segment can be regarded as a trapezoid as shown in Fig. 1 [31]. The frequency of serration is the number of segments produced per unit time, therefore it can be expressed as Eq. 7 [20].

$$f = \frac{V \sin \varphi}{d} \quad (7)$$

where  $d$  is the pitch of serrated chip as shown in Fig. 1. From metallurgical observation in the serrated chip, the chip segmentation is characterized by the degree of segmentation expressed as Eq. 8 [17].

$$G_s = (h_1 - h_2)/h_1 \quad (8)$$

where  $G_s$  is the degree of segmentation,  $h_1$  is the maximum height of the serrated chip, and  $h_2$  is the height of the continuous part of the serrated chip shown in Fig. 1.

On the basis of metallurgical observation in the serrated chip, it is found that the deformation in the serrated chip is different from that in the continuous chip [31–34]. The serrated chip segment EFGH is transformed from the parallelogram ABCD. Therefore, considering the change of AB in the cutting process, the model of serrated chip formation is shown in Fig. 2.

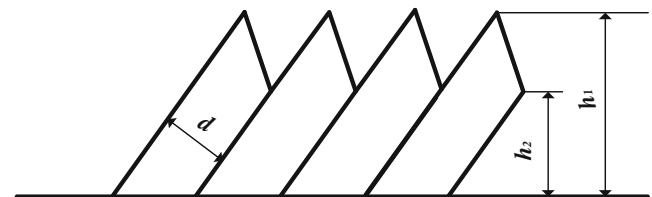


Fig. 1 Diagram of the serrated chip

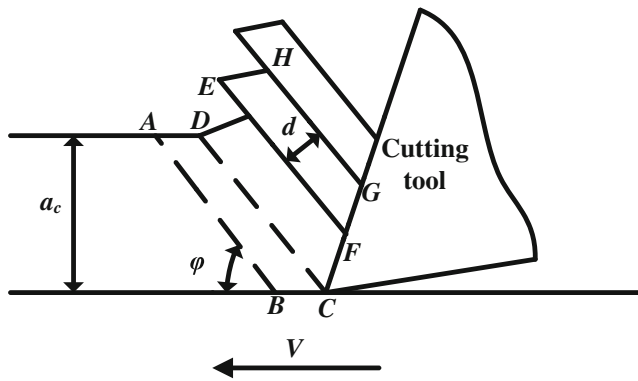


Fig. 2 Formation model of the serrated chip

The deformation in the serrated chip can be defined as Eqs. 9 and 10.

$$\gamma_{se} = \frac{|l_{EF} - l_{CD}|}{l_{BC} \sin \varphi} \tag{9}$$

$$\dot{\gamma}_{se} = \frac{\gamma_{se}}{\Delta t} \tag{10}$$

where  $\gamma_{se}$  is the shear strain of the serrated chip,  $\dot{\gamma}_{se}$  is the shear strain rate of the serrated chip,  $l_{EF}$  is the length of CD after deformation,  $l_{CD}$  is the length of CD,  $l_{BC}$  is the length of BC and  $\Delta t$  is the required cutting time to produce a serrated chip segment. It is assumption that the volume of the material during the deformation is const. That is  $S_{ABCD} = S_{EFGH}$ , so the  $l_{BC}$  can be obtained as Eq. 11.

$$l_{BC} = \frac{d(l_{EF} + l_{GH})}{2a_c} \tag{11}$$

The  $\Delta t$  can be expressed as following.

$$\Delta t = \frac{l_{BC}}{V} \tag{12}$$

By the geometric relationship, the  $l_{CD}$  can be expressed as Eq. 13.

$$l_{CD} = \frac{a_c}{\sin \varphi} \tag{13}$$

Submitting Eqs. 11, 12, and 13 into Eqs. 9 and 10, the deformation in the serrated chip can be expressed as the following:

$$\gamma_{se} = \frac{2a_c |l_{EF} \sin \varphi - a_c|}{d(l_{EF} + l_{GH}) \sin^2 \varphi} \tag{14}$$

$$\dot{\gamma}_{se} = \frac{4a_c^2 V |l_{EF} \sin \varphi - a_c|}{d^2 (l_{EF} + l_{GH})^2 \sin^2 \varphi} \tag{15}$$

Table 1 Chemical composition of 1045 steel

Element	C (%)	Si (%)	Mn (%)	Cr (%)	Ni (%)	Cu (%)
Wt.%	0.42–0.50	0.17–0.37	0.50–0.80	≤0.25	≤0.30	≤0.25

### 3 Experimental work and results

The high-speed cutting experiment was performed on a DAEWOO ACE-V500 vertical machining center. A 90° SN slot milling cutter (Kennametal, 4.96164-210) was used in the cutting experiment with coated carbide (KC110M) inserts whose type is SNHX12L5PZTNGP. The chemical composition of 1045 steel is presented in Table 1. The workpiece material under the heat treatment of quenching is used in the experiment. The diagram of workpiece is shown in Fig. 3. The thickness of workpiece is 2 mm. The hardness of the workpiece is measured with 200HRS-150 Rockwell hardness tester. As shown in Fig. 3, the measurement of workpiece hardness is carried out along MN at ten points and along OP at five points. Repeated this method three times, the average hardness of the workpiece is 38–42 HRC. 1045 steel was machined at the cutting speeds of 100, 200, 400, 600, 800, 1,000, 1,300, 1,600, 1,900, 2,200, 2,500, 3,200, and 3,600 m/min while the feed per tooth is 0.1 mm/z. The axial depth of cut above all is 2 mm.

The chips under different cutting speeds have been collected after machining. Through inlay, polishing, and washing with alcohol and water, the chips are observed in VHX-600 ESO digital microscope. The result shows that at the cutting speeds of 100, 200, and 400 m/min, the chip type is continuous. At the cutting speeds of 600, 800, 1,000, 1,300, 1,600, 1,900, and 2,200 m/min, the chip type changes to the serrated chip. At the cutting speeds of 2,500, 3,200, and 3,600 m/min, the chip changes to segmented one. The micrograms of different chip types are shown in Figs. 4, 5, and 6. The enlarged segmented chip is as shown in the upper right corner of Fig. 6.

The chip thicknesses of the continuous chip and the parameters  $h_1$ ,  $h_2$ ,  $l_{EF}$ ,  $l_{GH}$ , and  $d$  of the serrated chip are

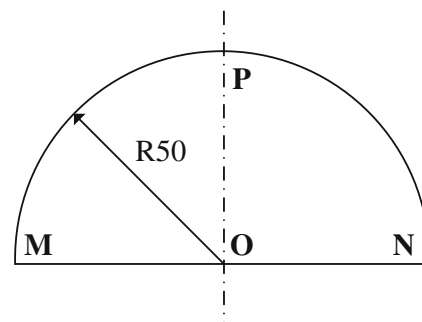


Fig. 3 Diagram of workpiece



**Fig. 4** Micrography of the continuous chip ( $V=100$  m/min)

measured in VHX-600 ESO digital microscope. The method of measurement is shown as Fig. 7, and every parameter is measured five times to take the average value. Submitting the chip thicknesses into Eqs. 1, 2, 5, and 6, the shear strain and the shear strain rate of the continuous chip under different cutting speeds are obtained.

The shear angles  $\varphi$  of the serrated chip can be obtained by using the method described in [35]. Submitting these parameters  $h_1$ ,  $h_2$ ,  $l_{EF}$ ,  $l_{GH}$ ,  $d$ , and  $\varphi$  into Eqs. 7, 8, 14, and 15, the frequency of serration, the degree of segmentation, the shear strain, and the shear strain rate of the serrated chip under different cutting speeds are obtained. The curves of the shear strain, the shear strain rate, the frequency of serration, and the degree of segmentation with the cutting speed are presented in Figs. 8, 9, 10, and 11. From these figures it is found that the shear strain, the shear strain rate, the frequency of serration, and the degree of segmentation all increase with the cutting speed.

From Fig. 8 it is shown that the relationship between the shear strain and the cutting speed under different chip types

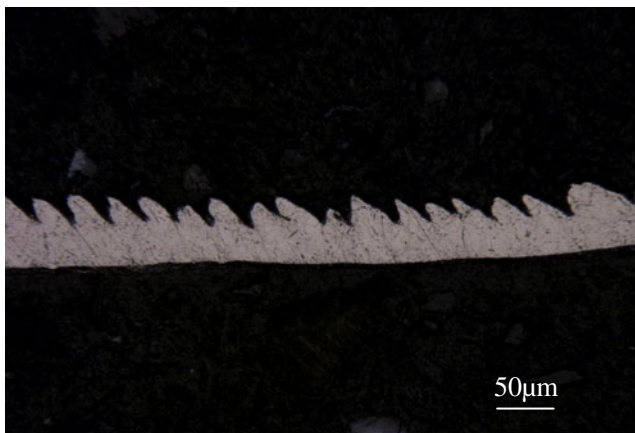


**Fig. 5** Micrography of the serrated chip ( $V=1,900$  m/min)

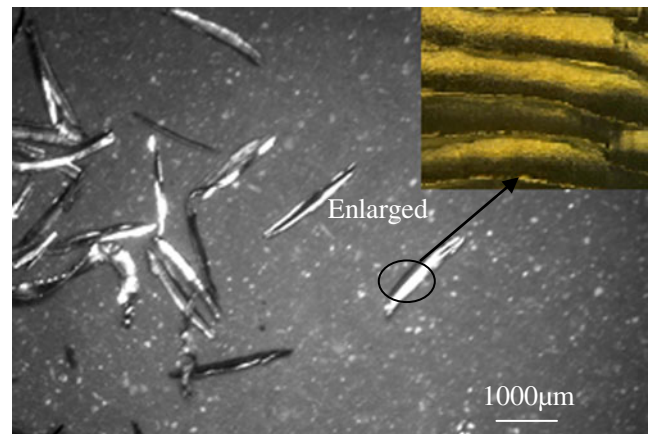


**Fig. 6** Micrography of the segmented chip ( $V=3,200$  m/min)

is different. While the chip type is continuous, the quantitative relation between the shear strain and the cutting speed can be expressed as Eq. 16.1. While the chip type is serrated, it can be expressed as Eq. 16.2. From Eqs. 16.1 and 16.2, it is proclaimed that the growth rate of the shear strain with the cutting speed while the chip type is serrated is faster than that of the continuous.

$$\gamma \propto V^{0.18} \quad (16.1)$$

$$\gamma \propto V^{0.40} \quad (16.2)$$

Figure 9 shows that the growth rate of the shear strain rate with the cutting speed while the chip type is serrated is faster than that of the continuous. While the chip type is continuous, the quantitative relation between the shear strain rate and the cutting speed can be expressed as Eq. 17.1.

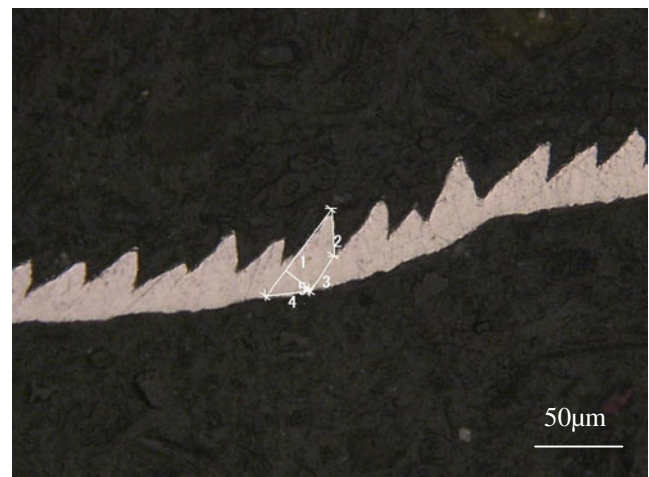


**Fig. 7** Micrography of the serrated chip measurement ( $V=2,200$  m/min)

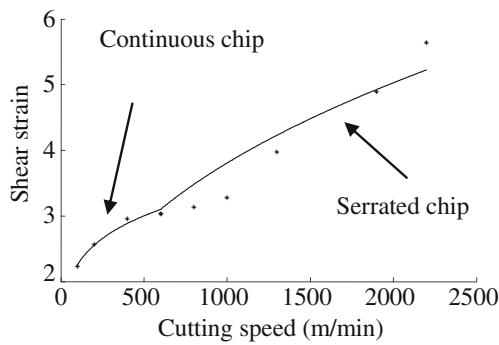


**Fig. 8** Shear strain as a function of cutting speed for a tool rake angle  $0^\circ$

While the chip type is serrated, it can be expressed as Eq. 17.2.

$$\dot{\gamma} \propto V^{1.12} \tag{17.1}$$

$$\dot{\gamma} \propto V^{1.88} \tag{17.2}$$

The differences between the serrated and the continuous chip are the frequency of serration and the degree of segmentation. From Figs. 10 and 11, the quantitative relation between the frequency of serration, the degree of segmentation, and the cutting speed can be expressed as Eqs. 18 and 19.

$$f \propto V^{1.34} \tag{18}$$

$$G_s \propto V^{1.57} \tag{19}$$

From Eqs. 16.1, 16.2, 17.1, and 17.2, it is found that the influence of cutting speed on the shear strain rate is greater than that on the shear strain during the continuous chip formation. The influence degree of cutting speed on the serrated chip deformation is greater than that of continuous chip. As the deformation increases, the shear strain hardening and the shear strain rate

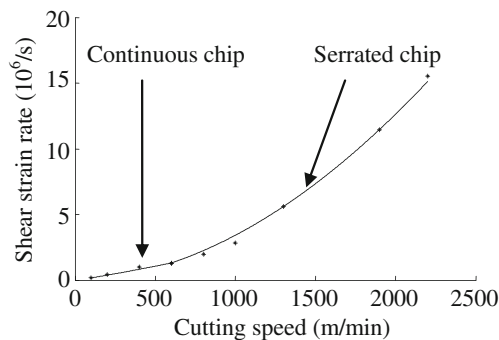


**Fig. 9** Shear strain rate as a function of cutting speed for a tool rake angle  $0^\circ$

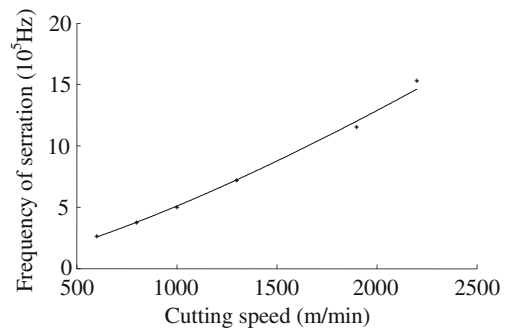


**Fig. 10** Frequency of serration as a function of cutting speed for a tool rake angle  $0^\circ$

hardening will increase the flow stress of the workpiece material in the shear zone. At the same time, the increasing of the chip deformation leads to the temperature rising in the shear zone. This phenomenon could promote the workpiece material softening. The combined action of the shear strain hardening, shear strain rate hardening, and thermal softening lead to adiabatic shearing in the shear zone. From Eqs. 16.1, 16.2, 17.1, 17.2, 18, and 19, the size of influence degree of the cutting speed on these parameters is in the following: the shear strain rate, the degree of segmentation, the frequency of serration, and the shear strain.

#### 4 Conclusion

The characterization of chip formation in machining 1045 steel is classified into that of the continuous and serrated chip formation. The characterization of the continuous chip formation is regarded as the chip deformation and that of the serrated chip formation is expressed as the frequency of serration, the degree of segmentation, and the deformation of serrated chip. Through machining 1045 steel, the chips under different conditions have been collected. The conclusions are that:

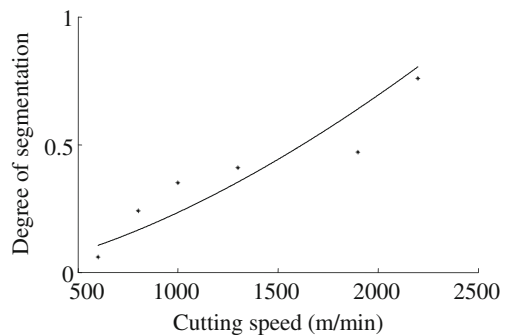


**Fig. 11** Degree of segmentation as a function of cutting speed for a tool rake angle  $0^\circ$

1. The shear strain and shear strain rate both increase with the cutting speed in continuous chip formation. The influence of the cutting speed on the shear strain rate is more sensitive than that on the shear strain.
2. An analytical serrated chip deformation model is established.
3. The frequency of serration, the degree of segmentation, the shear strain rate, and the shear strain all increase with the cutting speed during the serrated chip formation. The quantitative relations between these parameters and the cutting speed are obtained. The sensitivity of influence of the cutting speed on these parameters is in the following: the shear strain rate, the degree of segmentation, the frequency of serration, and the shear strain.

**Acknowledgments** The authors would like to thank the National Basic Research Program of China (2009CB724401), National Natural Science Foundation of China (50935003 and 50975162), Foundation of Shandong Province of China for Distinguished Young Scholars (JQ200918), and the Major Science and Technology Program of High-end CNC Machine Tools and Basic Manufacturing Equipment (2011ZX04016-031) for the financial support.

## References

1. Ernst H (1938) Physics of metal cutting. ASM 1–34
2. Merchant ME (1945) Mechanics of the metal cutting process. I. Orthogonal cutting and a type 2 chip. *J Appl Phys* 16(5):267–275
3. Sandstrom DR, Hodowany JN (1998) Modeling the physics of metal cutting in high-speed machining. *Mach Sci Technol* 2(2):343–353
4. Davim JP, Maranhão C (2009) A study of plastic strain and plastic strain rate in machining of steel AISI 1045 using FEM analysis. *Mater Des* 30(1):160–165
5. Shaw MC, Vyas A (1993) Chip formation in the machining hardened steel. *CIRP Ann Manuf Technol* 42(1):29–33
6. Elbestawi MA, Srivastava AK, El-Wardany TI (1996) A model for chip formation during machining of hardened steel. *CIRP Ann Manuf Technol* 45(1):71–76
7. Joshi SS, Ramakrishnan N (2001) Micro-structural analysis of chip formation during orthogonal machining of Al/SiCp composites. *J Eng Mater Technol* 123(3):315–321
8. Komanduri R, Brown RH (1981) On the mechanics of chip segmentation in machining. *J Eng Ind* 103:33–51
9. Ramesh A, Melkote SN, Allard LF, Riestler L, Watkins TR (2005) Analysis of white layers formed in hard turning of AISI 52100 steel. *Mater Sci Eng A* 390:88–97
10. Vyas A, Shaw MC (1999) Mechanics of saw-tooth chip formation in metal cutting. *J Manuf Sci Eng* 121(2):163–172
11. Barry J, Byrne G (2002) The mechanisms of chip formation in machining hardened steels. *J Manuf Sci Eng* 124(3):528–535
12. Puerta Velásquez JD, Bolle B, Chevrier P, Geandier G, Tidu A (2007) Metallurgical study on chips obtained by high speed machining of a Ti-6 wt.%Al-4 wt.%V alloy. *Mater Sci Eng A* 452–453:469–474
13. Poulachon G, Moisan A, Jawahir IS (2001) On modelling the influence of thermo-mechanical behavior in chip formation during hard turning of 100Cr6 bearing steel. *CIRP Ann Manuf Technol* 50(1):31–36
14. Poulachon G, Moisan AL (2000) Hard turning: chip formation mechanisms and metallurgical aspects. *J Manuf Sci Eng* 122(3):406–412
15. Su G, Liu Z (2010) An experimental study on influences of material brittleness on chip morphology. *Int J Adv Manuf Technol* 51:87–92
16. Ai X (2003) Technology of high speed cutting. National Defense Industrial Press, Beijing
17. Schulz H, Abele E, Salm A (2001) Material aspects of chip formation in HSC machining. *CIRP Ann Manuf Technol* 50(1):45–48
18. Zhu HT, Zbib HM, Aifantis EC (1995) On the role of strain gradients in adiabatic shear banding. *Acta Mech* 111(1–2):111–124
19. Aifantis EC (1992) On the role of gradients in the localization of deformation and fracture. *Int J Eng Sci* 30(10):1279–1299
20. Molinari A, Musquar C, Sutter G (2002) Adiabatic shear banding in high speed machining of Ti-6Al-4V: experiments and modeling. *Int J Plast* 18(4):443–459
21. Wright TW, Ockendon H (1992) A model for fully formed shear bands. *J Mech Phys Solids* 40(6):1217–1226
22. Dinzart F, Molinari A (1998) Structure of adiabatic shear bands in thermo-viscoplastic materials. *Eur J Mech A Solids* 17(6):923–938
23. Davies MA, Burns TJ, Evans CJ (1997) On the dynamics of chip formation in machining hard metals. *CIRP Ann Manuf Technol* 46(1):25–30
24. Pawade RS, Sonawane HA, Joshi SS (2009) An analytical model to predict specific shear energy in high-speed turning of Inconel 718. *Int J Mach Tools Manuf* 49(12–13):979–990
25. Huang J, Kalaitzidou K, Sutherland JW, Aifantis EC (2007) Validation of a predictive model for adiabatic shear band formation in chips produced via orthogonal machining. *J Mech Behav Mater* 18(4):243–264
26. Duan C, Wang MJ (2004) Adiabatic shear bands in 30CrNi3MoV structural steel induced during high speed cutting. *J Mater Sci Technol* 20(6):775–778
27. Moufki A, Molinari A, Dudzinski D (1998) Modeling of orthogonal cutting with a temperature dependent friction law. *J Mech Phys Solids* 46(10):2103–2138
28. Tay AO, Stevenson MG, de Vahl DG, Oxley PLB (1976) A numerical method for calculating temperature distributions in machining, from force and shear angle measurements. *Int J Mach Tool Des Res* 16(4):335–349
29. Komanduri R, Schroeder TA (1986) On shear instability in machining a nickel-iron base superalloy. *Trans ASME J Eng Ind* 108:93–100
30. Calamaz M, Coupard D, Nouari M, Girot F (2011) Numerical analysis of chip formation and shear localisation processes in machining the Ti-6Al-4V titanium alloy. *Int J Adv Manuf Technol* 52:887–895
31. He N, Lee TC, Lau WS, Chan SK (2002) Assessment of a deformation of a shear localized chip in high speed machining. *J Mater Process Technol* 129(1–3):101–104
32. Turley DM, Doyle ED, Ramalingam S (1982) Calculation of shear strains in chip formation in titanium. *Mater Sci Eng* 55(1):45–48
33. Duan CZ, Wang MJ, Pang JZ, Li GH (2006) A calculational model of shear strain and strain rate within shear band in a serrated chip formed during high speed machining. *J Mater Process Technol* 178(1–3):274–277
34. Yang Q, Liu Z, Cao C, Du J (2011) Strain and strain rate of serrated chip generated by high speed cutting of superalloys. *Trans Chin Soc Agric Mach* 42(2):225–228
35. Cotterell M, Byrne G (2008) Dynamics of chip formation during orthogonal cutting of titanium alloy Ti-6Al-4V. *Ann CIRP Manuf Technol* 57(1):93–96